Direct measurement of the low temperature spin state transitions in $La_{1-x}Sr_xCoO_3$ (0.05 < x < 0.3)

A. Gulec,[1,] and R.F. Klie,[1]

[1]*Department of Physics, University of Illinois at Chicago, Chicago, 60607, USA*

Sr-doped $LaCoO_3$ has a complex magnetic phase diagram, which is believed to be directly correlated to changes in the crystal structure and ordering of the Co^{3+} spin states. In this work, we study the low temperature Co^{3+}-ion spin state transitions in Sr-doped $LaCoO_3$ around the critical doping concentration using electron energy-loss spectroscopy of the O *K*-edge combination with Co *L*-edge fine structure. We measure the local spin state of the Co^{3+}-ions and we demonstrate that the Co^{3+} spin-state transition only occurs in $La_{0.95}Sr_{0.05}CoO_3$ single -crystal materials in the temperature range accessible by LN_2 in-situ cooling, while no structural symmetry change is observed. The presence of this low-temperature spin-state transition in $La_{1-x}Sr_xCoO_3$ (x<0.17) has been proposed as the origin of the percolative magnetic ordering in doped $LaCoO_3$

I. INTRODUCTION

Primarily due to their exceptional magnetic transitions which are related to changes the Co^{3+}-ion spin states, $LaCoO_3$-based perovskite oxides (see Figure 1a) have been studied for a long time. More specifically, bulk $LaCoO_3$ shows two temperatures dependent transitions occurring below 100 K and above 500 K. Below 100 K bulk $LaCoO_3$ exhibits nonmagnetic behavior while after the first transition it becomes a semiconducting insulator and after the second transition above 500 K, it turns metallic[1,2]. Both transitions are believed to be the result of changes in the Co-ion spin states. These spin states transitions are related to the competition between the crystal-field splitting (Δ_{CF}) of the Co *3d states* into e_g and t_{2g} orbitals, which encourages the lower spin states, and the Hund's exchange rule, which is responsible for higher spin configurations. The first magnetic transition[2,3,4] is believed to be due to a change in the Co^{3+}-ion spin state from a low spin- LS ($t^{6}_{2g}\, e^{0}_{g}\, S=0$) state to combination of the high

spin-HS ($t^4_{2g}\, e^2_g\, S=2$) and LS states[5] or alternatively an intermediate spin ($t^5_{2g}\, e^1_g\, S=1$) IS state.[6,7,8] The high-temperature transition stems from a change in the Co^{3+}-ion spin-state from the IS state or combination of LS and HS states to HS state. Figure 1b shows the electronic configuration of the Co 3*d* orbitals and possible spin configurations. Due to the relatively small difference between the crystal-field splitting energy (Δ_{CF}) and the intra-atomic Hund`s rule exchange energy, magnetism can be tuned in various ways including: i) changing the particle size of powder sample[9], ii) epitaxial tensile strain via the properly chosen substrate,[10,11] iii) external pressure[12] or iv) doping with a alkaline-earth ion, such as Sr, having a different ionic radius.

Bulk $La_{1-x}Sr_xCoO_3$ (LSCO) has been intensively studied by various techniques, such as Extended X-ray Absorption Fine Structure (EXAFS), Neutron Pair Distribution Function (PDF)[13], NMR[14,15], Small-Angle Neutron Scattering (SANS)[16], and Inelastic Neutron Scattering (INS), Electron Spin Resonance (ESR)[17]. It was reported that with increasing Sr-doping, $La_{1-x}Sr_xCoO_3$ changes from a non-magnetic insulator which undergoes a thermally induced Co^{3+} ion spin state transition at low temperature, to a spin glass at low Sr-doping and a ferromagnet at higher doping. As the Sr-doping concentration increases, spin polarons which are caused by substituting divalent Sr^{2+} ions for trivalent La^{+3} ions merge and form short-range FM clusters, since the neighboring mixed valance Co ions interact ferromagnatically via double exchange mechanism[15]. At the critical doping of $x \approx 0.17$, the clusters percolate, leading to a crossover from short- to long-range FM and the system simultaneously undergoes a percolative insulator-to-metal transition (IMT)[15].

Using EXAFS and neutron PDF measurements, *Sunduram et al.*[13] reported large Jahn-Teller distortions of the Co-O bond in Sr-doped $LaCoO_3$ samples with doping concentrations as high as 35%. However, intermediate spin states, corresponding to the presence of singly occupied Co e_g orbitals was not observed. *Smith at al*[14,15] utilized NMR and theoretical modeling to show that the Co ion spin state

transition coincides with nanoscale hole–poor regions of the inhomogeneous doped $LaSrCoO_3$. For lightly hole doped $LaCoO_3$, *Podlesnyak et al*[17] conclude that INS, ESR and NMR data provide evidence for two regimes, one dominated by spin polarons at low temperature and one by thermally activated magnetic Co^{3+} dominated at higher temperature. However, all these studies mentioned above rely on probe sizes that could be significantly large than the nano-scale feature they are trying to characterize. Aberration corrected transmission electron microscopy can provide sub-Angstrom spatial resolution with in-situ cooling capabilities and sufficient energy resolution to resolve the local doping and spin state variations.

Recently, atomically resolved Z contrast imaging combining with electron energy loss spectroscopy (EELS) has been used to examine electronic and magnetic properties of epitaxial $LaCoO_3$ thin films [18,18,19]. For example, *Kwon et al.*[18] and *Biškup et a*[19]*l* report the presence of a superstructure, which shows itself as dark stripes, is found in epitaxially strained $LaCoO_3$ thin film grown on $SrTiO_3$ substrate. Using electron energy-loss spectroscopy (EELS) of the cobalt *L*-edges and oxygen *K*-edges, *Kwon et al.*[16] conclude that the superstructure is caused by cobalt spin state ordering rather than the oxygen vacancy ordering previously reported in $SrCoO_3$[20] as well as strained $LaCoO_3$. However, both oxygen vacancies and changes in the Co-ion spin states result in similar changes in the oxygen K-edge fine-structure and a systematic study of the effects of hole doping on the local Co-ion spin state transition has not yet been reported. Moreover, the effects of hole doping on the O K-edge pre-peak intensity, as well as the local Co-ion spin state will lay the foundation for any future work focusing on the spatial distribution of magnetic clusters near the critical hole doping concentration of 17%.

In this work, we will use high-angle annular dark field (HAADF) imaging in combination with electron diffraction, angular-resolved EELS, and *in situ* cooling experiment in an aberration-corrected scanning transmission electron microscope (STEM), the UIC JEOL ARM200CF, to study $LaCoO_3$

single-crystals with 5%, 17% and 30% Sr doping. We will demonstrate that by using these techniques which provide local probe, only $La_{0.95}Sr_{0.05}CoO_3$ single-crystal samples exhibits the signs of a low temperature spin-state transition upon *in-situ* cooling that was previously observed in NMR measurements of spin relaxation rates.[14]

II. EXPERIMENTAL DETAILS

The single-crystal $La_{1-x}Sr_xCoO_3$ bulk samples, which were grown by floating zone methods, are provided by J.T Mitchell from Argonne National Laboratory.[14] Previous electron diffraction studies confirmed the single crystal nature of the materials and the absence of any secondary phases. The TEM samples are prepared by standard wedge polishing and ion mill procedure using a 3kV Ar^+-ion beam. The JEM-ARM200CF is equipped with a probe aberration corrector, a cold field emission source allowing for 0.35eV energy resolution and a Gatan Enfina electron energy loss spectrometer. The EELS experiments are performed in TEM diffraction mode with a selected area aperture allowing us to confine the probe to an area with a radius of approximately 50 nm. All EELS data is acquired in the [001] pseudo-cubic crystal orientation to avoid any orientation dependence of the EELS near-edge fine structure. The exponential EEL spectrum background is subtracted from each spectrum and the resulting data is normalized with respect to the post edge intensity. The *in-situ* cooling experiments are performed by using the Gatan double-tilt liquid nitrogen (LN_2) cooling stage (model 636 cryogen). During the cooling experiment the sample experiences special drifting and other mechanical instabilities. The objective lens creates a local magnetic field of several Tesla and will contribute to spin alignment of the sample during the STEM measurements. For STEM high angle annular dark field (HAADF) imaging, a 90 mrad inner collection angle and a convergence semi-angle of 22 mrad (for 40 μm aperture) are used.

III. RESULTS AND DISCUSSION

Figure 2 shows selected area electron diffraction patterns (SADP) taken from the three different samples in the [1 1 0] orientation at room and LN_2 temperatures. The effects of *in-situ* cooling are shown in green and red for room and LN_2 temperature, respectively, with the overlap region shown in white and the background in blue. None of the samples are found to have any kind of structural phase transition during cooling experiment. The 5% and 17% doped samples show an isotropic increase in the diffraction patterns at low temperature, corresponding to an overall shrinkage in crystal structure volume, while the 30% Sr-doped sample shows no detectable change in the diffraction patterns. A comparison of the diffraction patterns for all three doping concentration at room temperature is also shown in Figure 2d) and reveals that the overall unit cell volume increases with the increase in Sr-doping from 5% to 30%. This is consistent with previous reports for the parent $LaCoO_3$ and different amount of *Sr* doping concentrations.[21, 22, 23]

Atomic-resolution high-angle annular dark-field (HAADF) STEM images of single crystal $La_{1-x}Sr_xCoO_3$ in the pseudo cubic [1 1 0] orientation are shown in Figure 3, both at room temperature and at liquid nitrogen temperature. Since the HAADF image contrast is highly sensitive to atomic columns with higher Z elements, imaging of oxygen columns cannot be achieved due to its low atomic number, *Z*, and screening effects of heavier neighboring atoms. In Figure 3, the lower image intensity stems from the Co atomic columns while higher intensity columns consist of La\Sr atoms. The image resolutions appear worse during *in-situ* cooling due to mechanical instabilities associated with LN_2 boiling off and spatial sample drift. For $x=0.05$, we show a TEM high-resolution phase-contrast image instead of a

HAADF and the Co column not resolved here. In the single crystal samples studied here, we do not observe any superstructure at either room temperature or at low temperature, such as darker or lighter stripes which were reported earlier for $LaCoO_3$ thin films on different substrates due to the presence of spin state or vacancy ordering. However, having extra spots at diffraction pattern at $\left[\frac{1}{2}\ -\frac{1}{2}\ \frac{1}{2}\right]$ in the pseudo-cubic directions for all doped samples, as seen in Figure 2 at both temperature and low temperature can be interpreted as a modulation in the size of unit cell projection at pseudo cubic [1 1 0] orientation which can be the result of CoO_6 octahedral distortion. Since TEM and HAADF imagining techniques used here are not sensitive to imaging light elements, such as oxygen, we are not able to confirm or quantify this distortion. However, we have not observed any structural symmetry change as a function of temperature other than the overall decrease in unit cell volume based on our electron diffraction analysis.

It has been shown that electron energy-loss (EEL) spectroscopy of the O K-edge can be utilized to measure the Co-ion spin-state transitions by quantifying the O K-edge pre-peak intensity[7]. In addition, the transition metal L_2 and L_3 edges, which are results of transition of an electron from the transition metal *2p* states to unoccupied *3d* orbitals, can be utilized to determine the occupancy of the transition metal *3d* orbitals[24 10]. While the L_3/L_2 intensity ratio, or so called white line ratio, is an indication of valance states of Co atoms, the energy resolution of non-monochromated electron guns is not sufficient to resolve changes due to spin-state transitions of the Co ions. X-ray absorption spectroscopy has demonstrates the ability to resolve those changes, but suffers from significantly lower spatial resolution.[5]

Figure 4 shows the EEL spectra of single-crystal $La_{1-x}Sr_xCoO_3$ samples oriented in the pseudo cubic [1 1 0] direction, both at room temperature and liquid nitrogen temperatures. In Figure 4 a-c), the O *K*-edges is shown at room temperature (solid line) and liquid nitrogen temperature (dashed line), exhibiting three peaks near the edge onset, labeled *a, b* and *c*. We used these peaks to identify a possible Co-ion spin state transition as a function of temperature and Sr-doping. The O K-edge intensity is normalized

to the continuum intensity above 560 eV. The O K-edge pre-peak, labeled *a*, stems from the hybridization of *O 2p* with *Co 3d*, whereas peaks *b* and *c* can be assigned to the hybridization of *O 2p* with *La 5d* and *Co 4sp*, respectively. At room temperature, the increase in the Sr-doping concentration increases the Co^{4+} concentration resulting in an increased number of available Co 3d states, which manifests itself as a relative increase in the *O K*-edge pre-peak intensity, as seen in Figure 4. At low temperature, there is an increase in pre-peak intensity, labeled *a*, for 5% doped sample while a similar change is not observed for critically doped, 17% sample and for the 30% doped sample. This observed increase in the pre-peak intensity can be either due to the creation of oxygen vacancies or any change in the electron distribution at Co e_g and t_{2g} orbitals which origins a Co-ion spin state transition. However, the *Co L*-edge structure, which is sensitive to the valence state of the Co atom, and thus also the presence of Co or O vacancies, does not indicate any significant change at room and LN_2 temperature not only for 5% doped sample but all other doping concentrations as shown in lower corner of Figure 4 for each sample.

Assuming that the stoichiometry of the samples remains unchanged during the in-situ cooling experiments, one can explain the change in the O K edge pre-peak intensity as the follows: In the low spin-state configuration, the Co^{3+} e_g energy levels are solely responsible for the pre-peak intensity, since all the t_{2g} orbital are filled with the $3d^6$ electrons. On the other hand, in the higher spin-state configurations, while the Co oxidation state remains unchanged, the Co e_g energy levels are not completely empty, thus reducing the number of available states for excited electrons in the e_g orbital while simultaneously increasing the number of available t_{2g} orbitals. Therefore, one should expect an increase in the O K-edge pre-peak intensity at low temperature for samples that have undergone a transition to the Co-ion low spin-state. We conclude that the observed decreased intensity of O *K*-edge pre-peak in the sample doped with 5% Sr is due to a thermally induced Co-ion spin state transition, similar to that reported in undoped $LaCoO_3$.[7]

Kwon et a[18] reported that spin state ordering in $LaCoO_3$ film grown on $SrTiO_3$ substrate results a superstructure of ordered darker stripes found perpendicular to film/substrate interface, and concluded that the increased atomic distances in the dark stripes are responsible for smaller hybridization between *Co* and O atoms, and, therefore, for a higher Co-ion spin state. Moreover, this structural change also lowers the peak ***c*** of the O K-edge, which stems from the hybridization between spherically symmetric *O s* state and *Co d* states. However, in the data shown in here, we do not observe any crystal symmetry change other than the decrease in unit cell volume as the result on *in-situ* cooling. If the change in the O *K*-edge fine structure was purely structural, then we should have seen an increase in intensity of peak ***c*** through cooling in both 17% and 5% doped samples as a result of the decrease in the unit-cell volume at lower temperature. However, the intensity of peak *c* remains unchanged in the 5% doped sample, while a decrease is seen at low temperature for the 17% doped sample. Therefore, we can conclude that this spin state transition is temperature driven rather than structural, since the change in exchange energy is more dominant than the change in the crystal splitting as the result of sample cooling. On the other hand, not having the spin-state transition at higher doping concentration (e.g. 17% and 30%) can be explained by the fact that a single La^{3+} atom has 8 *Co* neighbors which will be affected the substitution with a divalent Sr atom. Thus, increasing the doping concentration from 5% to 17% will increase the number of the Co^{4+} ions in a higher spin state converted by Sr^{+2} so that the doping-driven spin state transition to higher spin state is dominant and the thermally driven spin-state transition can no longer be observed.

IV. CONCLUSION

In summary, with a local probe provided by STEM and EELS techniques, we find a Co-ion spin state transition in 5% doped $La_{1-x}Sr_xCoO_3$ through in-situ cooling experiments, while 17% and 30% doped samples do not show any indication for such transitions. In samples below the critical doping concentration of x=17%, atomic resolved HAADF images and SADP do not show any indication of a

changes in crystal structure symmetry during the in-situ cooling which can possibly be responsible of the observed changes in the *O K*-edge fine-structure. For higher doping concentration, such as the 17% and 30% doped samples studied here, the doping driven spin state transition is dominant over thermally driven spin state transition at low temperature. These results now allow us to distinguish for the effects of oxygen vacancy ordering from Co-ion spin state ordering, as previously reported for $LaCoO_3$ thin films. This will be essential in studying the percolative nature of the magnetic ordering in hole-doped LaCoO3 samples both thin films, as well as single crystal. It was previously suggested that the phase transition in Sr-doped $LaCoO_3$ is associated with merging of magnetically ordered clusters of the length-scale of a few unit cells. Due to the lack of spatial resolution of many magnetic probes, EELS in a STEM appears to be the ideal candidate to study this transition and the work reported here lays the foundation for such an experiment. Using the reported changes in the O K-edge pre-peak intensity and the anti-correlation with the Co $L_{3,2}$-ratio, the spin state transition can now be clearly distinguished from a change in local Co valence due to oxygen vacancies or local chemical inhomogeneities.

ACKNOWLEDMENT

The authors want to thank J.F. Mitchell for providing the Sr-doped single crystal samples and C. Leighton for the stimulating discussions. This work was supported by a grant from the National Science Foundation (Grant No. DMR-0846748). The acquisition of the UIC JEOL JEMARM200CF was supportred by a NSF MRI-R^2 grant (DMR-0959470).Support from the UIC Research Resources Center (RRC), in particular A.W. Nicholls is acknowledged.

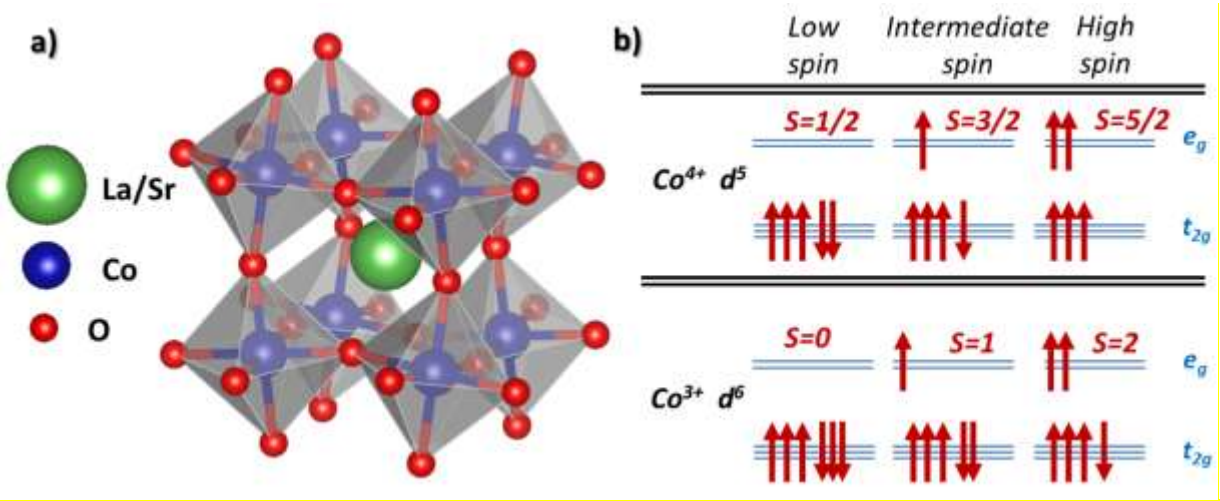

FIG. 1. a) Crystal structure of $La_{1-x}Sr_xCoO_3$. b) Possible electronic configuration of Co 3d states orbitals and spin state configurations.

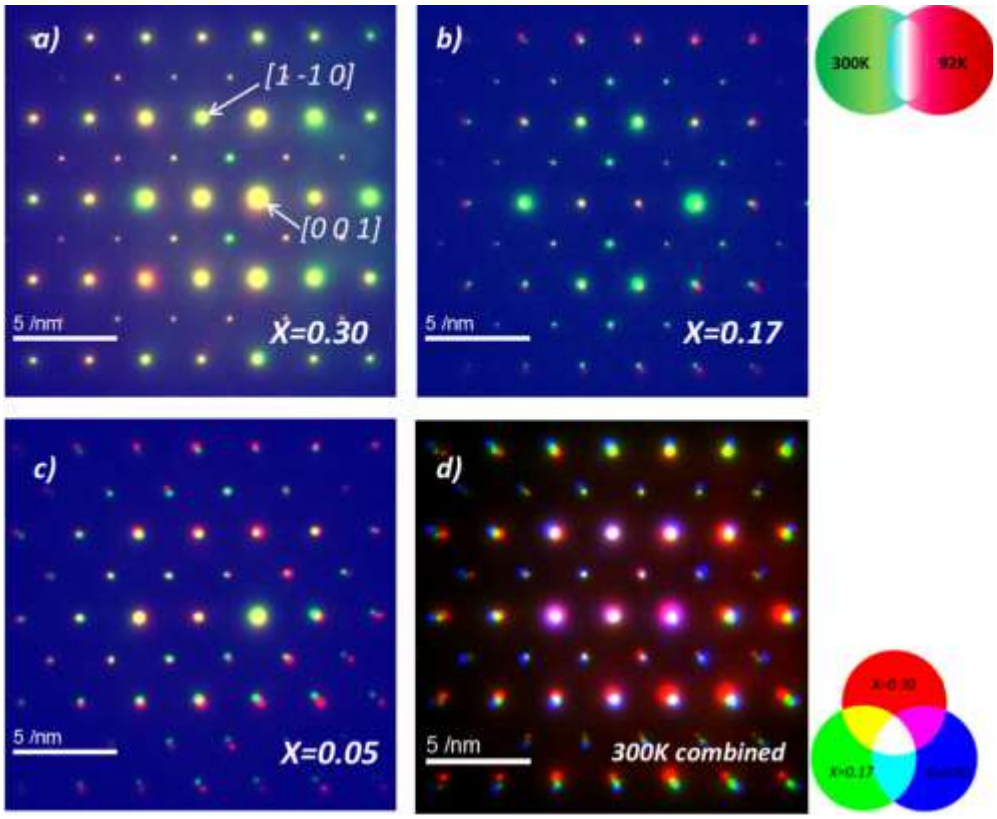

FIG. 2. Combined selected area diffraction pattern (SADP) of $La_{1-x}Sr_xCoO_3$ at room temperature (RT) in green color and liquid nitrogen temperature (LNT) in red color after in situ cooling in [0 1 1] direction *a) for x=0.30 b) x=0.17* and *c) x=0.05*. *d)* SADP of three samples combined in room temperature in same orientation where x=0.30, x=0.17 and x=0.05 are shown in red , green and blue, respectively.

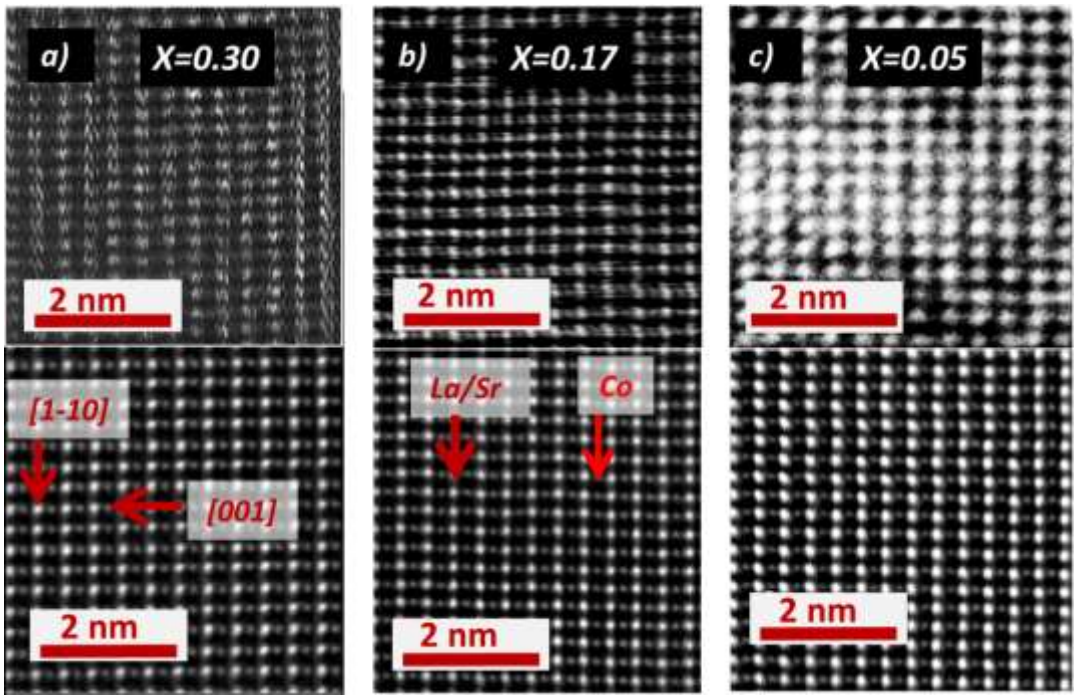

FIG. 3. HAADF images taken at [1 1 0] pseudo cubic orientation at LNT at the top and HAADF images taken at RT in the bottom in the same orientation are shown for *x=0.30, x=0.17* and *x=0.05* respectively.

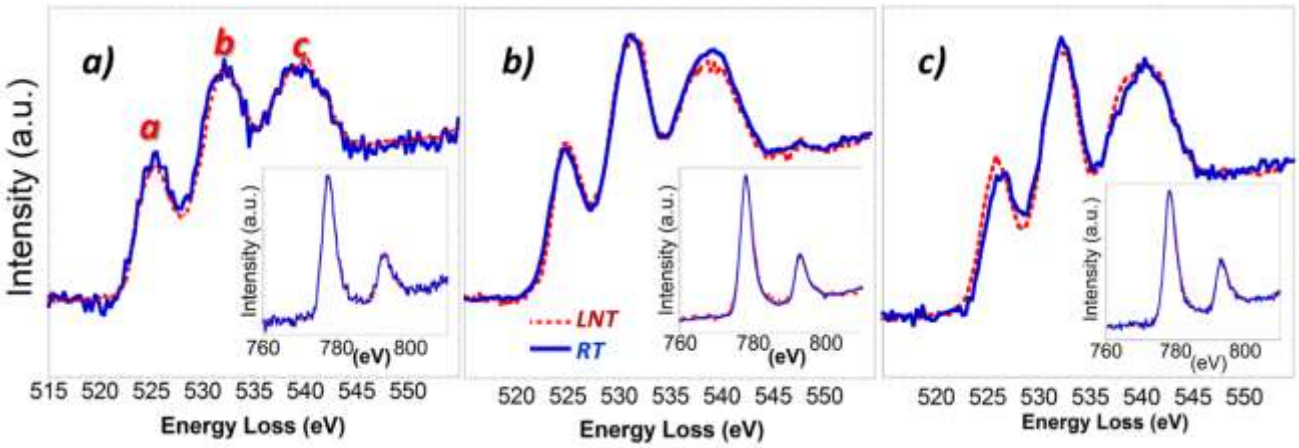

FIG. 4. EEL Spectra of O K edge taken in room temperature in solid line and liquid nitrogen temperature in dashed line of ***a)*** $La_{0.70}Sr_{0.30}CoO_3$ $La_{0.95}Sr_{0.05}CoO_3$, ***b)*** $La_{0.83}Sr_{0.17}CoO_3$ and ***c)*** $La_{0.95}Sr_{0.05}CoO_3$. Similarly EELS data of *Co L* edges both at room temperature and at liquid nitrogen temperature for each sample is inserted at right lower corner.

REFERENCES

[1] R.R. Heikes, R.C. Miller, and R. Mazelsky, Physica **30** (8), 1600 (1964).

[2] John B. Goodenough, Journal of Physics and Chemistry of Solids **6** (2–3), 287 (1958).

[3] P. M. Raccah and J. B. Goodenough, Physical Review **155** (3), 932 (1967).

[4] M. A. Señarís-Rodríguez and J. B. Goodenough, Journal of Solid State Chemistry **118** (2), 323 (1995).

[5] M. W. Haverkort, Z. Hu, J. C. Cezar, T. Burnus, H. Hartmann, M. Reuther, C. Zobel, T. Lorenz, A. Tanaka, N. B. Brookes, H. H. Hsieh, H. J. Lin, C. T. Chen, and L. H. Tjeng, Physical Review Letters **97** (17), 176405 (2006).

[6] M. A. Korotin, S. Y. Ezhov, I. V. Solovyev, V. I. Anisimov, D. I. Khomskii, and G. A. Sawatzky, Physical Review B **54** (8), 5309 (1996).

[7] R. F. Klie, J. C. Zheng, Y. Zhu, M. Varela, J. Wu, and C. Leighton, Physical Review Letters **99** (4), 047203 (2007).

[8] R. F. Klie, J. C. Zheng, Y. Zhu, M. Varela, J. Wu, and C. Leighton, Phys. Rev. Lett. **99**, 047203 (2007).

[9] I. Fita, V. Markovich, D. Mogilyansky, R. Puzniak, A. Wisniewski, L. Titelman, L. Vradman, M. Herskowitz, V. N. Varyukhin, and G. Gorodetsky, Physical Review B **77** (22), 224421 (2008).

[10] R. F. Klie, T. Yuan, M. Tanase, G. Yang, and Q. Ramasse, Applied Physics Letters **96** (8), 082510 (2010).

[11] D. Fuchs, C. Pinta, T. Schwarz, P. Schweiss, P. Nagel, S. Schuppler, R. Schneider, M. Merz, G. Roth, and H. v. Lohneysen, Physical Review B (Condensed Matter and Materials Physics) **75** (14), 144402 (2007).

[12] J. S. Zhou, J. Q. Yan, and J. B. Goodenough, Physical Review B **71** (22), 220103 (2005); M. Lugovy, V. Slyunyayev, N. Orlovskaya, D. Verbylo, and M. J. Reece, Physical Review B **78** (2) (2008).

[13] N. Sundaram, Y. Jiang, I. E. Anderson, D. P. Belanger, C. H. Booth, F. Bridges, J. F. Mitchell, Th Proffen, and H. Zheng, Physical Review Letters **102** (2), 026401 (2009).

[14] R. X. Smith, M. J. R. Hoch, W. G. Moulton, P. L. Kuhns, A. P. Reyes, G. S. Boebinger, H. Zheng, and J. F. Mitchell, Physical Review B **86** (5), 054428 (2012).

[15] R. X. Smith, M. J. R. Hoch, P. L. Kuhns, W. G. Moulton, A. P. Reyes, G. S. Boebinger, J. Mitchell, and C. Leighton, Physical Review B **78** (9), 092201 (2008).

[16] C. He, S. El-Khatib, J. Wu, J. W. Lynn, H. Zheng, J. F. Mitchell, and C. Leighton, EPL (Europhysics Letters) **87** (2), 27006 (2009).

[17] A. Podlesnyak, M. Russina, A. Furrer, A. Alfonsov, E. Vavilova, V. Kataev, B. Büchner, Th Strässle, E. Pomjakushina, K. Conder, and D. I. Khomskii, Physical Review Letters **101** (24), 247603 (2008).

[18] Ji-Hwan Kwon, Woo Seok Choi, Young-Kyun Kwon, Ranju Jung, Jian-Min Zuo, Ho Nyung Lee, and Miyoung Kim, Chemistry of Materials **26** (8), 2496 (2014).

[19] Neven Biškup, Juan Salafranca, Virat Mehta, Mark P. Oxley, Yuri Suzuki, Stephen J. Pennycook, Sokrates T. Pantelides, and Maria Varela, Physical Review Letters **112** (8), 087202 (2014).

[20] Y. Ito, R. F. Klie, N. D. Browning, and T. J. Mazanec, Journal of the American Ceramic Society **85** (4), 969 (2002).

[21] Y. J. Yoo, K. K. Yu, J. Y. Kim, Y. P. Lee, K. W. Kim, and K. P. Hong, Physica B: Condensed Matter **385–386, Part 1** (0), 411 (2006).
[22] V. V. Sikolenko, A. P. Sazonov, I. O. Troyanchuk, D. Többens, U. Zimmermann, E. V. Pomjakushina, and H. Szymczak, Journal of Physics: Condensed Matter **16** (41), 7313 (2004).
[23] C. He, S. Eisenberg, C. Jan, H. Zheng, J. F. Mitchell, and C. Leighton, Physical Review B **80** (21), 214411 (2009).
[24] Z. L. Wang, J. Bentley, and N. D. Evans, Micron **31** (4), 355 (2000).

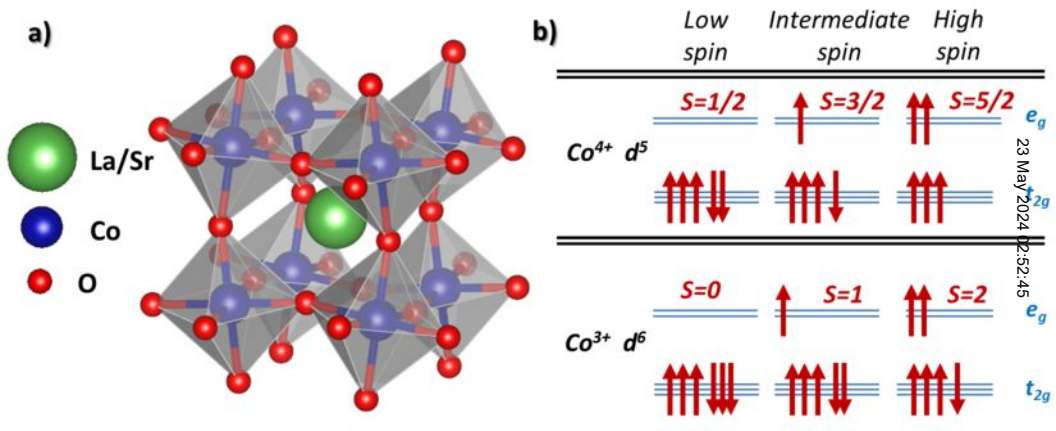

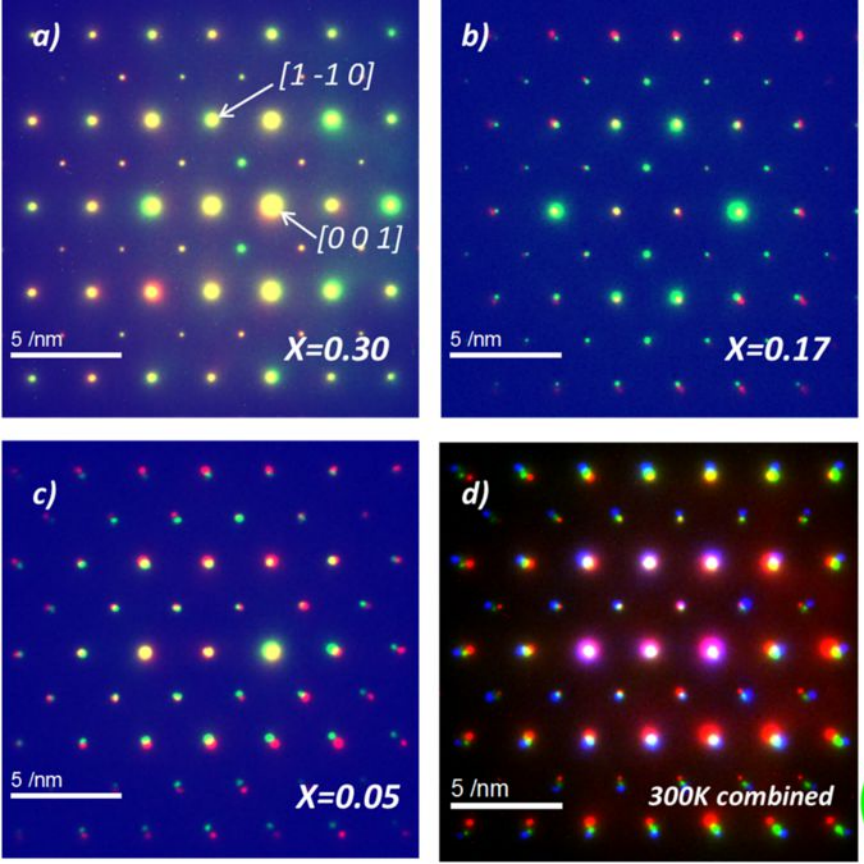

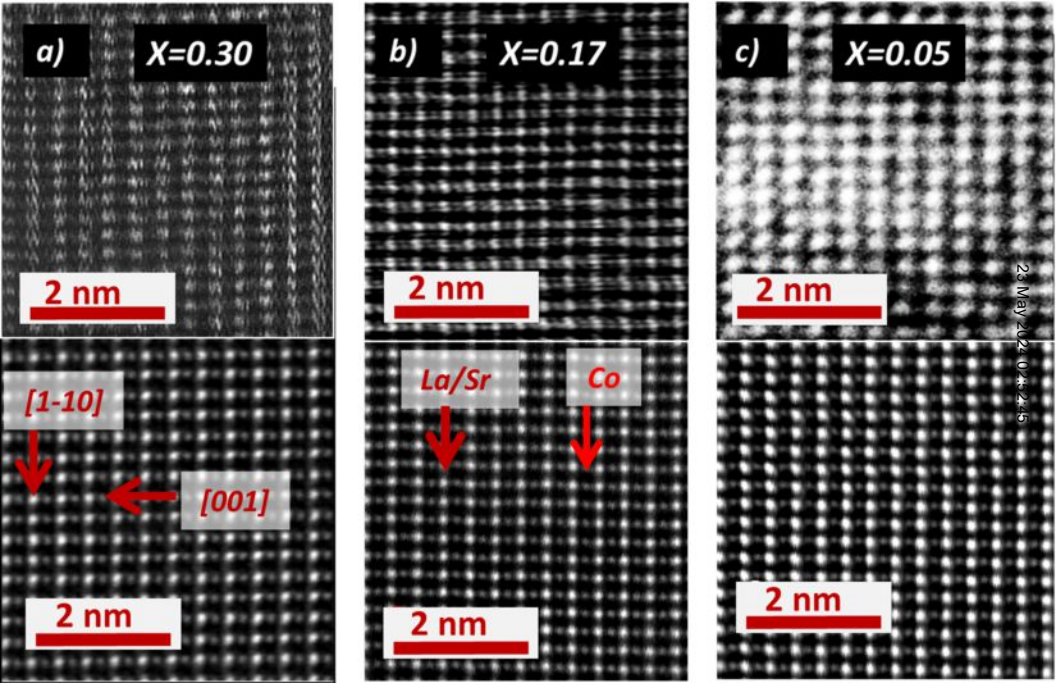
a)
X=0.30
2 nm
[1-10]
[001]
2 nm
b)
X=0.17
2 nm
La/Sr
Co
2 nm
c)
X=0.05
2 nm
2 nm